1974

Telluric current survey over two known geothermal areas

Robert Glen Hawe
The University of Montana

A TELLURIC CURRENT SURVEY OVER TWO KNOWN GEOTHERMAL AREAS

By

Robert Glen Hawe

B.A., University of Montana, 1966

Presented in partial fulfillment of the requirements for the degree of

Master of Science in Geology

UNIVERSITY OF MONTANA

1974

Approved by:

Gary W. Crosby
Chairman, Board of Examiners

John M. Stewart
Dean, Graduate School

May 29, 1974
Date

ProQuest LLC.
789 East Eisenhower Parkway
P.O. Box 1346
Ann Arbor, MI 48106 - 1346

ACKNOWLEDGMENTS

I would like to take this opportunity to thank the following people for their participation in preparing this thesis. My father, Glen Hawe, who inspired me to become a geologist; my advisors, Dr. Robert Weidman and Dr. Gary Crosby, who offered guidance and counseling throughout my academic endeavors; and my friend, Dorothy Dryden, who has assisted me in preparing several publications, including this thesis.

LIST OF FIGURES

Figure

TABLE OF CONTENTS

CHAPTER I

THE PROBLEM AND ITS SIGNIFICANCE

Geothermal energy sources may play a major role in satisfying the future power requirements of the world. In 1971 White *et al.* classified geothermal systems as either vapor-dominated hydrothermal systems or hot water systems. The Geysers in California, the Mud Volcano area in Yellowstone National Park and the area near Larderello, Italy, are classified as vapor-dominated or dry steam systems. Hot water systems are much more common and are usually found in either permeable sedimentary or volcanic rocks or competent rocks such as granite. The competent rocks maintain channels for fluid migration along faults or fractures. If the temperature equals 150°C, this type of system has a high potential for self-sealing by deposition of SiO_2 minerals along the fractures. A characteristic of these systems appears to be relatively low maximum temperatures. In areas where they have been drilled, the temperature increases with depth up to a maximum of approximately 250°C. Drilling to greater depths yields little or no increase in temperatures. Camas Hot Springs, at Hot Springs, Montana, appears to be a hot water system where the maximum temperature found to date is 53°C at a depth of 74 meters (244 feet).

A third type of geothermal anomaly is hot dry rocks, probably associated with a cooling magma chamber where the heat has not been transferred to ground water (Blackwell, 1973). This type of system

may exist near Marysville, Montana, where there is a high heat flow without surface manifestations. Blackwell and Baag (1973) derived three models for a magma chamber buried beneath the surface thermal anomaly near Marysville, Montana, using a diffusivity of 0.015 cm^2/sec. These models define spherical magma chambers buried at depths of 1 km (3281 ft) to 1.5 km (4921 ft) with radius of 4 km (13,124 ft) and 3 km (9843 ft), respectively.

To date geothermal areas have been found by surface observations of features such as fumarole activity, geysers, and hot springs. These areas have then been mapped by geochemical and geophysical techniques. The geophysical studies generally applied to geothermal areas include seismic (mainly recording ground noise and micro-earthquakes), thermal (temperature gradient and heat flow), gravity, magnetics, and electrical (resistivity mapping and depth sounding).

Since the resistivity of rocks decrease with water content, porosity, temperature, and salinity, electrical geophysical methods have been utilized for investigating many geothermal areas throughout the world. The parameter temperature, unique to geothermal fields, will produce a ten-fold decrease in resistivity as it increases from 25°C to 400°C with all other parameters remaining constant.

Resistivity studies made over geothermal areas of the world have utilized various electrode configurations. Schlumberger arrays were used on the Monte Amiata geothermal field in Italy (Calamai *et al.*, 1970) the Tatum Volcanic Regions of Taiwan (Cheng, 1970), and in the Imperial Valley of California (McEuen, 1970;

Meidav, 1970). The Wenner and dipole-dipole electrode configurations were used for horizontal profiling in the Broadlands Geothermal Region of New Zealand (Risk, 1970). The Marysville Geothermal Area was mapped using a dipole-dipole electrical array (Jackson, 1972). These studies all found resistivity anomalies associated with thermally active areas. The above studies used man-induced electrical signals for determining resistivity. A magnetotelluric survey was conducted in New Zealand using natural earth or telluric currents generated by lightning discharges as the signal source (Keller, 1970). This study showed a resistivity contrast between thermal and non-thermal areas of at least a factor of 10 similar to other resistivity surveys.

Explorations for geothermal areas require depth penetration of 1 km (3281 ft) to 3 km (9843 ft). At these depths, standard resistivity measurements using various electrode arrays require great lengths of wire and large power plants. For this reason, utilization of natural earth currents (telluric currents) as a signal source would have a distinct advantage providing, of course, that the data can be correctly interpreted.

Telluric and magnetotelluric methods of exploration were compared at a frequency of 8 Hz over several known mineral deposits in Canada (Slankis *et al.*, 1972). This study indicated that the two methods generated similar results if in the case of the telluric survey, the resistivity at a base station was determined by some independent absolute measuring technique. The magnetotelluric

study made in New Zealand at a frequency of 35 Hz produced a resistivity anomaly comparable with results obtained by conventional resistivity survey over a known geothermal area (Keller, 1970). Since telluric techniques have not been applied to geothermal explorations, the objective of this study was to develop necessary instrumentation and a telluric current survey technique to answer the following questions. First, can this type of system generate a useful apparent resistivity map at the depths required for mapping geothermal areas? Second, can a realistic model of geothermal areas be drawn from the data by applying a multiple frequency technique, similar to that used in a magnetotelluric survey which generated a pseudo depth profile over a known mineral deposit (Strangway *et al.*, 1973)?

CHAPTER II

TECHNOLOGY AND INSTRUMENTATION

Telluric currents at frequencies greater than 1 Hz are generated by lightning discharges and industrial noise from power distribution systems (Keller, Frischknecht, 1970). These signals have a peak amplitude at 8 Hz due to the earth and ionosphere acting as a resonate cavity (Schuman, 1952), and after a decrease in amplitude at approximately 11 Hz continue to increase up to a maximum between 7 to 10 kHz. The energy radiated at this latter maximum results from the components of the stepped leader in a cloud-to-ground lightning discharge and the return stroke that follows it (Gupta *et al.*, 1972; Kimpara, 1965). This signal propagates in the form of a ground wave and a sky wave (Gallenberger, 1970). The maximum distance this signal has been recorded from its point of origin is 2000 km (1242 miles) (National Bureau of Standards, 1960). At frequencies less than 1 kHz, the mode of propagation is solely in the form of a ground wave. At distances greater than 300 km (186 miles), the magnitude of sferics signals remains relatively constant due to the influence of the ionosphere (Horner, 1964).

Natural earth currents have been used in mineral exploration to depths of several hundred feet and petroleum exploration to depths of 914 meters (3000 ft) to 1219 meters (4000 ft) (Slankis *et al.*, 1972; Yungul *et al.*, 1973). The effective depth of penetration for these signals is a function of frequency and resistivity as defined by the skin depth equation: (Strangway *et al.*, 1973)

$$d = \sqrt{\frac{\rho}{\pi \mu f}}$$

where

d = skin depth in meters

ρ = resistivity in ohm meters

μ = permeability in henries/meter

or $\mu = 1.27 \times 10^{-6}$ henries/meter

$$d = 503.8 \sqrt{\frac{\rho}{f}} \qquad \text{Equation (1)}$$

where d is defined as the depth in meters to where the amplitude of the signal is 1/e of the surface amplitude.

This study used the above equations as a formulation to develop a technique for obtaining an apparent resistivity profile at depths of several kilometers by measuring natural earth signals at several selected frequencies. The frequencies selected were 8 Hz, 70 Hz, 700 Hz, and 7000 Hz. The 8 Hz signal is the signal propagated in the first Schumann resonance mode which has the maximum energy of the four Schumann resonance frequencies (Schumann, 1952).

70 Hz was selected since its energy source is a combination of lightning and commercial 60 Hz power. This signal has the maximum strength of the four selected frequencies.

700 Hz is simply an intermediate frequency with atmospherics from lightning discharges as its source. Of the four frequencies selected for this study, 700 Hz has the minimum signal strength.

7000 Hz is near the peak energy emitted by the return stroke in

lightning discharges. The energy level at the selected frequencies is approximately independent of the distance to the energy source providing that source is at least 300 km (186 miles) from the measuring station. This characteristic makes it possible to abandon continuous operation of a base station at many locations on the earth during a major portion of the year.

In nearly any survey, location and time of day or year will not have an appreciable effect on the strength of the 70 Hz and 7000 Hz signals. 70 Hz signals have a depth penetration in material with resistivities of 100 ohm meters or greater of at least 600 meters (1968 ft) making this a desirable frequency for mapping deep resistivity anomalies. 7000 Hz signals penetrate the subsurface having resistivities of 100 ohm meters or greater to a depth of 60 meters(196 ft). This depth is desirable for mapping near surface anomalies.

Electrical resistivity measurements made in the Mud Volcano area of Yellowstone National Park found that a vapor-dominated geothermal system is characterized by a high resistivity anomaly at depth due to the presence of dry steam overlain by a layer of low resistivity. The low resistivity is a result of steam condensing into hot water (Zohdy, 1973). The depth of the low resistivity layer was 91 meters (300 ft) to 121 meters (400 ft). Providing the above resistivity anomalies characterize vapor-dominated geothermal systems, one would expect a telluric survey that utilized 70 Hz and 7000 Hz to show high and low resistivity anomalies, respectively, which would suggest a more detailed investigation of that area.

Figure 1 shows the skin depth in meters for each of the four frequencies at any value for resistivities up to 10,000 ohm meters. This graph was generated by the skin depth equation.

The instrument used for this study integrated the A.C. components of signals generated at the four separate frequencies described above. These signals were amplified, filtered, and rectified prior to integration. The time in seconds required for the integrated signal to obtain an arbitrary meter value of 1 was recorded at each frequency. If the resistivity was known at a base station, the resistivity could be determined at any location by the following equation:

$$t_1\rho_{a1} = t_2\rho_{a2} \quad \text{or} \quad \rho_{a2} = \frac{t_1\rho_{a1}}{t_2} \qquad \text{Equation (2)}$$

where

t_1 = integration time at the base station

ρ_{a1} = apparent resistivity at the base station

t_2 = integration in time at the new station

ρ_{a2} = apparent resistivity at the new station

Since the magnitude of the telluric current signals vary with frequency due to the nature of their origin, an instrument calibration constant K_f can be added to the equation.

$$\rho_{a2} = K_f \frac{t_1\rho_{a1}}{t_2} \qquad \text{Equation (3)}$$

where

K_f = meter calibration constant for each frequency.

The calibration constants for this study were determined by averaging several measurements at different locations randomly distributed over a known Cretaceous granodiorite stock (Blackwell, 1973). The assumption used for this calibration was that the resistivity of the stock was approximately 1000 ohm meters and that this stock had a constant resistivity to depths of at least 6000 meters (1968 ft). The constant K_f was determined at each frequency such that equation (3) gave values of 1000 ohm meters at all frequencies.

The instrument used in these surveys is a relative measuring device; therefore, absolute resistivity values for a base station must be determined independently by other electrical techniques. Alternatively, since in a preliminary survey, one is interested more in resistivity anomalies than absolute resistivity, it is often feasible to assume an apparent resistivity value based on surface geology such as outcropping rocks, lake beds, etc. Under these conditions one must assign a value for the 7000 Hz frequency only, which investigates the shallow subsurface, and calculate the resistivities at the other frequencies by use of the calibration constants determined for each meter under controlled conditions. The field procedure for using this instrument utilizes two electrodes separated a distance of 7.6 meters (25 ft) to 60 meters (200 ft). The separation distance determines the signal strength and not the depth of penetration. These electrodes can be oriented in any direction but that direction should be used for the entire study.

Surveys using this instrument simply record the integration period at the four frequencies over each station simultaneously with the base station. During this study it was found that the integration times over the base station fluctuated by less than a factor of 2 over a period of several days. Since this is within the degree of accuracy one would expect for this type of reconnaissance survey, it was determined unnecessary to monitor the base station continuously. It is, however, recommended that the base station be visited several times daily to insure that the integration periods are not changing.

CHAPTER III

SURVEYS

A survey designed to evaluate the telluric method for geothermal application included mapping and profiling the geothermal areas at Camas Hot Springs, Montana, and the "blind" heat flow anomaly near Marysville, Montana (Blackwell, 1973; Crosby, 1973). These sites were selected since each had previously been mapped geologically and geophysically. The geophysical surveys over these areas included gravity, magnetic, and resistivity plus heat flow and microearthquakes.

Hot Springs Survey

Camas Hot Springs lies near the contact of a Precambrian diorite sill and argillites of the Ravalli Group, a submember of the Precambrian Belt Super Group. The Belt Super Group in this area comprises of up to 15,239 meters (50,000 ft) of argillites, quartzites, and argillaceous limestones (Crosby, 1973). This entire sequence has been subjected to metamorphism of varying degrees and warped into broad open folds trending in a north south direction. The valleys in the survey area are filled with Glacial Lake Missoula sediments consisting of sequences of silts and clay to depths of up to 91 meters (300 ft). These sediments which thin at the valley margins rest on sand and gravel layers deposited on the coarse river flood plain deposits prior to the last advance of ice. A more detailed description of the local geology can be found in a preliminary report by Crosby (1974).

The Precambrian diorite sill is apparently non-magnetic since it did not generate a magnetic anomaly as can be seen in Figure 2. There is, however, a small magnetic anomaly near the hot springs between A-A' that lies at a depth determined by Peter's half slope method of approximately 182 meters (600 ft). Crosby suggests that this magnetic anomaly is caused by an igneous rock other than the Precambrian sill and that it is a possible heat source for the hot springs in this area.

Figure 3 is a copy of Crosby's (1973) gravity map. This map shows a series of faults in the immediate area of the hot springs. The map indicates that the hot springs rest on a bedrock-valley fill contact and that at the mouth of the valley, 1.6 km (1 mile) southeast of the springs, bedrock is approximately 701 meters (2300 ft) deep.

A Scintrex SEM-600 In Phase - Out of Phase instrument was used by Crosby over the immediate area of the hot springs for making a resistivity map. A copy of this map is shown in Figure 4. Depth of penetration was estimated at a maximum of 91 meters (300 ft). Examination of this map shows a resistivity of 100 ohm meters along the margins of the valley with a minimum resistivity of 10 ohm meters near its center. The station at the northeast corner of the map which measured 94 ohm meters was used as the base station for the telluric current survey.

The map shown in Figure 5 was generated by measuring telluric currents at a frequency of 70 Hz. The survey was conducted with a 30 meters (100 ft) dipole separation. Each measurement was taken with the dipole oriented in a north south direction. During the initial portion of the survey, the base station marked B. S. was monitored continuously. The measurements were made using radio communications to transmit a start command. At this command, both stations would begin integration. The time required for each to integrate a meter reading of 1 was recorded. The ratio of these times was used to determine the apparent resistivity of the station. It was found unnecessary to maintain a continuously monitored base station because during the period of investigation it drifted by less than a factor of 2. This was within the accuracy expected for this technique. The base station was checked at least 3 to 4 times daily after continuous monitoring was no longer used. Each measurement was made at least 3 times to insure that the integration was not performed during a period when a sporadic burst of energy was transmitted from some nearby source.

The resistivity map covers the same approximate area as Crosby's magnetic and gravity maps. Examination of this map shows one anomalous area near Camas Hot Springs that coincides with the magnetic high reported by Crosby. The low resistivity in the middle of the map running from the north to the northeast outlines the channel of water saturated lake sediments deposited by Glacial Lake Missoula. The

anomaly near the base station suggests the presence of a high resistivity intrusive at an approximate depth of 1900 meters (6233 ft).

This anomaly was examined in greater detail as shown in the cross section A-A' in Figure 6. Figure 6 shows the apparent resistivities beneath each station at the four measured frequencies - 7000 Hz, 700 Hz, 70 Hz, and 8 Hz. The station identified as H is located at the Hot Springs Bath House. The contours isolate sections of approximately the same apparent resistivity. The geologic model shown in Figure 7 is derived by applying the skin depth graph in Figure 1 to the resistivity versus frequency plot in Figure 6. The low resistivity found at 7000 Hz implies a water saturated clay and silt layer with a thickness near the center of the valley of 60 meters (200 ft) to 91 meters (300 ft) thinning to less than 15 meters (50 ft) near the hotel. This low resistivity layer rests on a bedrock consisting of undifferentiated Precambrian Belt rocks and the Precambrian dioritic sill. At a depth of approximately 304 meters (1000 ft), there is a high resistivity zone extending to a depth of approximately 1828 meters (6000 ft). This could be interpreted as a vapor-dominated reservoir similar to that reported at the Mud Volcano area in Yellowstone National Park (Zohdy, 1973). At a depth of approximately 1828 meters (6000 ft), a layer of rock that has a lower resistivity appears to be present. This could be an intrusive since its apparent resistivity is 1300 ohm meters. The south edge of the cross section appears to be faulted as suggested by the high resistivity values that extend downward to depths of several thousand feet.

Marysville Area Survey

The center of the Marysville heat flow anomaly lies approximately 4.8 km (3 miles) west of the old mining camp of Marysville. Bedrock outcrops throughout the area expose Precambrian sedimentary rocks, primarily the Empire Shale and the Helena Limestone. These rocks have been intruded by several systems of sills and dikes both before and after the emplacement of the Marysville stock. The stock is exposed to the east and southeast of the anomalous heat flow. Tertiary quartz porphyry stocks have been cut by diamond drill exploration programs conducted in the Empire Creek drainage near the proposed drill site. A more complete geologic history of the area can be found in Blackwell and Baag (1973).

A ground magnetic total field map shown in Figure 8 was made by Blackwell in 1973. This map suggests that there is nothing apparently magnetically anomalous associated with the high heat flow shown in Figure 9. Figure 9 is a heat flow and geothermal gradient map also produced by Blackwell in 1973. A residual gravity map generated by Blackwell in 1974 shows a gravity anomaly that reasonably outlines the high heat flow area. Dallas Jackson (1972) of the United States Geophysical Survey conducted a dipole-dipole resistivity survey in 1972. He found an area of low resistivity in the bottom of Empire Creek. This area has a resistivity of 150 ohm meters and lies over a portion of the high heat flow anomaly. In addition to the low resistivity anomaly, Jackson shows a small anomaly due east a

distance of approximately 1.6 km (1 mile) with a resistivity of 600 ohm meters and another small anomaly of 1000 ohm meters approximately 1.6 km (1 mile) to the southwest. In addition, resistivities of 400 and 500 ohm meters were found on each side but slightly north of the Bald Butte Area.

The telluric current survey was designed to cover approximately the same area as Blackwell's heat flow map. The study consisted of 100 stations randomly distributed over the area with a concentration of data points near the center of the highest heat flow readings.

Figure 10 is a resistivity map made at a frequency of 70 Hz. This map has two small isolated high resistivity anomalies. The small high through which cross sections A-A' and B-B' run is located approximately 402 meters (1/4 mile) due south of the proposed drill site which is located at point A. The other small high resistivity anomaly lies approximately 1.6 km (1 mile) due east of the drill site and corresponds with a similar anomaly reported by Jackson (1972). The area of high resistivity to the east and south are the result of intrusives associated with the Marysville stock. The high resistivity running along the west margin of the area has no surface manifestation that identifies its cause. At 70 Hz the effective depth of penetration at a resistivity of 100 ohm meters from the skin depth equation illustrated in Figure 1 is approximately 609 meters (2000 ft). For this reason, one would not necessarily expect a surface expression associated with all high resistivity

anomalies found at 70 Hz. Figure 11 is a resistivity map based on 7000 Hz telluric currents. At this frequency, the depth of penetration at a resistivity of 100 ohm meters is only 60 meters (200 ft) to 91 meters (300 ft). A close examination of this map shows the area of interest is again surrounded by high resistivity rocks to the east and south with a general decrease in resistivity towards the center apparently associated with the high heat flow. The low resistivity anomaly reported by Jackson (1972) appears at this frequency and seems to be associated with the valley fill along the bottoms of Empire Creek and Lost Horse Creek. Another low appears near the spring at the head of the small gulch running south of the drill site along the cross section A-A'. In general, it appears that the ridge in the center of the heat flow anomaly has a relatively high surface resistivity as suggested by the two isolated highs near the intersections under A-A' and B-B'. Figure 12 shows a resistivity cross section of A-A' with respect to frequency. The contours define areas of approximately the same resistivity. By applying depth with respect to resistivity and frequency to these zones, the pseudo geologic model shown in Figure 13 was constructed.

The low resistivity areas near the surface are the result of stream bottoms and springs, each of which are apparent at the surface. The two shallow (500 ohm meter) zones appear to rest on a lower resistivity layer which could possibly be the water table. Near A' the intrusive is exposed at the surface and the resistivity decreases

at a depth of approximately 152 meters (500 ft) where it remains relatively constant to depths of at least 3047 meters (10,000 ft).

The entire surface from the stock northward is underlain by a rock with a resistivity of approximately 350 ohm meters. Beneath this zone there is a layer with a marked decrease in resistivity. A small isolated plug with a resistivity of 100 ohm meters is centered near the small spring at the head of the gulch running south of the drill site. This plug appears to come within 914 meters (3000 ft) of the surface and could be the cause of the high heat flow anomaly.

Figure 14 shows the apparent resistivity at different frequencies along cross section B-B'. The contours isolate areas of approximately the same resistivity. By applying the skin depth equation to these values, the pseudo geologic model shown in Figure 15 was drawn. This profile was run along the 1767 meter (5800 ft) contour line on the Canyon Creek Quadrangle. There appears to be a rather uniform layer near the surface with a resistivity of approximately 400 ohm meters. A small area near the center of the profile has a lower resistivity perhaps resulting from ground water.

This high resistivity layer lies on a thick very low resistivity sequence similar to that found beneath cross section A-A' (Figure 13). This profile has two anomalous high's each small in diameter and coming to within approximately 457 meters (1500 ft) of the surface. The one near B appears to be associated with the similar plug found near A in Figure 13.

CHAPTER IV

CONCLUSIONS

This study measured telluric currents at different frequencies over two types of geothermal areas, the hot water type and the hot dry rock type. The frequencies used were 8 Hz, 70 Hz, 700 Hz, and 7000 Hz. These frequencies were selected due to the nature of their origin. If there is no electrical storm activity within a radius of approximately 300 km (186 miles) of the measuring station, the average amplitude of the earth currents should remain approximately constant provided that the integration period is 1 second or more. When making measurements, a stray high amplitude signal is obvious to the operator and will appear anomalous if three or more readings are taken at each station. Based on the above premises, this study was made without a continuous monitor at a base station. The base station, however, was checked at least three times each day that measurements were made. These continuous checks of the base station showed that signal amplitude varied no more than a factor of 2 over the entire duration of the survey.

The measuring equipment was calibrated for the different frequencies by assuming that the Marysville stock had a reasonably constant resistivity down to a depth of at least 6000 meters (19,686 ft).

This calibration established a constant for each frequency that was used for all measurements made at both of the study sites. The Hot Springs area was mapped at 70 Hz due to the low resistivity

of the lake deposits which covered a large portion of the area. These deposits had a resistivity of 10 to 50 ohm meters. A high resistivity anomaly was found near the Hot Springs Bath House which coincided with a magnetic anomaly. A multiple frequency profile across this anomaly generated a model of the subsurface that had a hot vapor-dominated zone overlying an intrusive approximately 304 meters (1000 ft) beneath the surface. An apparent fault on the southern flank of the anomaly could provide a channel for this hot water to migrate to the surface. Prior to reaching the surface, the water encounters a 91 meter (300 ft) thick clay cap which forces it along the clay bedrock contact causing it to surface near the Hot Springs Bath House.

The Marysville area was mapped at both 70 Hz and 7000 Hz. The 70 Hz map revealed a high resistivity anomaly immediately south of the proposed drill site. In addition, another small high resistivity anomaly was located approximately 1 mile due east. At least one or perhaps both of these anomalies may be responsible for the high heat flow in this area. The 7000 Hz map showed a resistivity low near the drill site which appears to follow the Empire Creek and Lost Horse Creek drainages. High resistivity anomalies were formed along the ridge line south of Empire Creek.

Two multiple frequency profiles were drawn through the anomalies. These profiles suggest that two small intrusives buried at a depth of approximately 761 meters (2500 ft) are the possible cause of the anomalies. The intrusives are surrounded by very low resistivity

rocks. This could imply hot dry rocks heated by the intrusives. The low resistivity zones are covered by a layer of rocks with a resistivity of 300 to 500 ohm meters. Near the surface there are low resistivity anomalies that appear to be the result of springs and stream drainages.

Realizing that these models were generated from apparent resistivity and that the depths and widths of anomalous bodies are approximate, they seem reasonable in view of known geophysics and geology. At Camas Hot Springs, a small magnetic anomally was found that coincides with the high resistivity anomally; both of these suggest the presence of a subsurface intrusive. Similarly the gravity map of this same area implies a fault trending in an east southeasterly direction that coincides with the apparent fault shown along the southern flank of the resistivity model in Figure 7. The heat flow models for a buried magma chamber derived by Blackwell (1973) are in excellent agreement with the resistivity models derived by this study for the Marysville area. They both suggest the presence of one or more heat sources, small in size and buried at a depth of approximately 914 meters (3000 ft). Surface features such as springs, lake beds, outcrops, intrusives, etc., were all apparent on the multiple frequency pseudo resistivity cross sections. In view of the above, this technique appears to provide a method for making deep apparent resistivity measurements at a reasonable cost and with a minimum amount of time and effort.

BIBLIOGRAPHY

Blackwell, David, and Baag, Czang-Go, 1973, Heat flow in a "blind" geothermal area near Marysville, Montana. Geophysics, v. 38, No. 5, p. 941-956.

Calamai, A., Cataldi, R., Squarci, P., and Taffi, L, 1970, Geology, geophysics, and hydrogeology of the Monte Amiata geothermal field. Geothermics, Spec. Issue, v. 1.

Cheng, W. T., 1970, Geophysical exploration in the Tatum Volcanic Region, Taiwan, Geothermics, Spec. Issue, v. 2, pt. 1, p. 262.

Crosby, G. W., 1974, Preliminary study of the Hot Springs, Montana, area. (Unpublished report).

Gallenberger, R. J., 1970, Sferic source location accuracy evaluation. Naval Electronics Laboratory Center, Propagation Tech. Div., San Diego, CA.

Gupta, S. P. Rao, Manoranjan, and Tantry, B. A. P., 1972, J. Geophys. Res. v. 77, No. 21, p. 3924.

Horner, F., and Bradley, P. A., 1964, The spectra of atmospherics from near lightning discharges. J. Atmos. Terr. Phys., v. 26, p. 1155-1166.

Jackson, D., 1972, Geophysical investigation of Marysville Geothermal area, The cross section. U. S. Geophysical Survey, v. 3, No. 11, p. 6.

Keller, G. V., 1970, Induction methods in prospecting for hot water. Geothermics, Spec. Issure, v. 2, pt. 1, p. 318.

Keller, George, and Frischknecht, Frank, 1970, Electrical methods of geophysical prospecting. Pergamon Press, New York.

Kimpara, A., 1965, Electromagnetic energy radiated from lightning. *In:* Problems of atmospheric and space electricity, Ed. E. Coroniti. Elsevier Publishing Company, p. 352-365.

McEuen, R. B., 1970, Delineation of geothermal deposits by means of long spacing resistivity and airborne magnetics. Geothermics, Spec. Issue, v. 2, pt. 1, p. 295.

Meidav, T., 1970, Application of electrical resistivity and gravimetry in deep geothermal exploration. Geothermics, Spec. Issue, v. 2, pt. 1, p. 303.

National Bureau of Standards, 1960, Daytime attenuation rates in the very low frequency band using atmospherics. Radio Sci. J. Res. G4D, p. 349-355.

Risk, G. F., MacDonald, W. J. P., and Dawson, G. B., 1970, DC resistivity surveys of the Broadlands geothermal region, New Zealand. Geothermics, Spec. Issue, v. 2, pt. 1, p. 287.

Schumann, W. O., 1952, The damping of electromagnetic oscillations characteristic of the earth-ionosphere system. Z. Naturforsch, 7 a 250-2.

Slankis, J. A., Telford, W. M., and Becker, A., 1972, 8-Hz telluric and magnetotelluric prospecting. Geophysics, v. 37, No. 5, p. 862.

Strangway, D. W., Swift, C. M., Jr., and Holmer, R. C., 1973, The application of audio-frequency magnetotelluric (AMT) to mineral exploration. Geophysics, v. 38, No. 6, p. 1159-1175.

White, D. E., Muffler, L. J. P., and Truesdell, A. H., 1971, Vapor-dominated hydrothermal systems compared with hot-water system. Econ. Geol., v. 66, p. 75-97.

Yungul, M. R., Hembrere, M. R., and Greenhouse, J. P., 1973, Telluric anomalies associated with isolated reefs in Midland Basin Texas. Geophysics, v. 38, No. 3, p. 545.

Zohdy, A. A. R., Anderson, L. A., and Muffler, L. J. P., 1973, Resistivity self potential and induced-polarization surveys of a vapor-dominated geothermal system. Geophysics, v. 38, No. 6, p. 1130-1144.

APPENDIX A

Figures

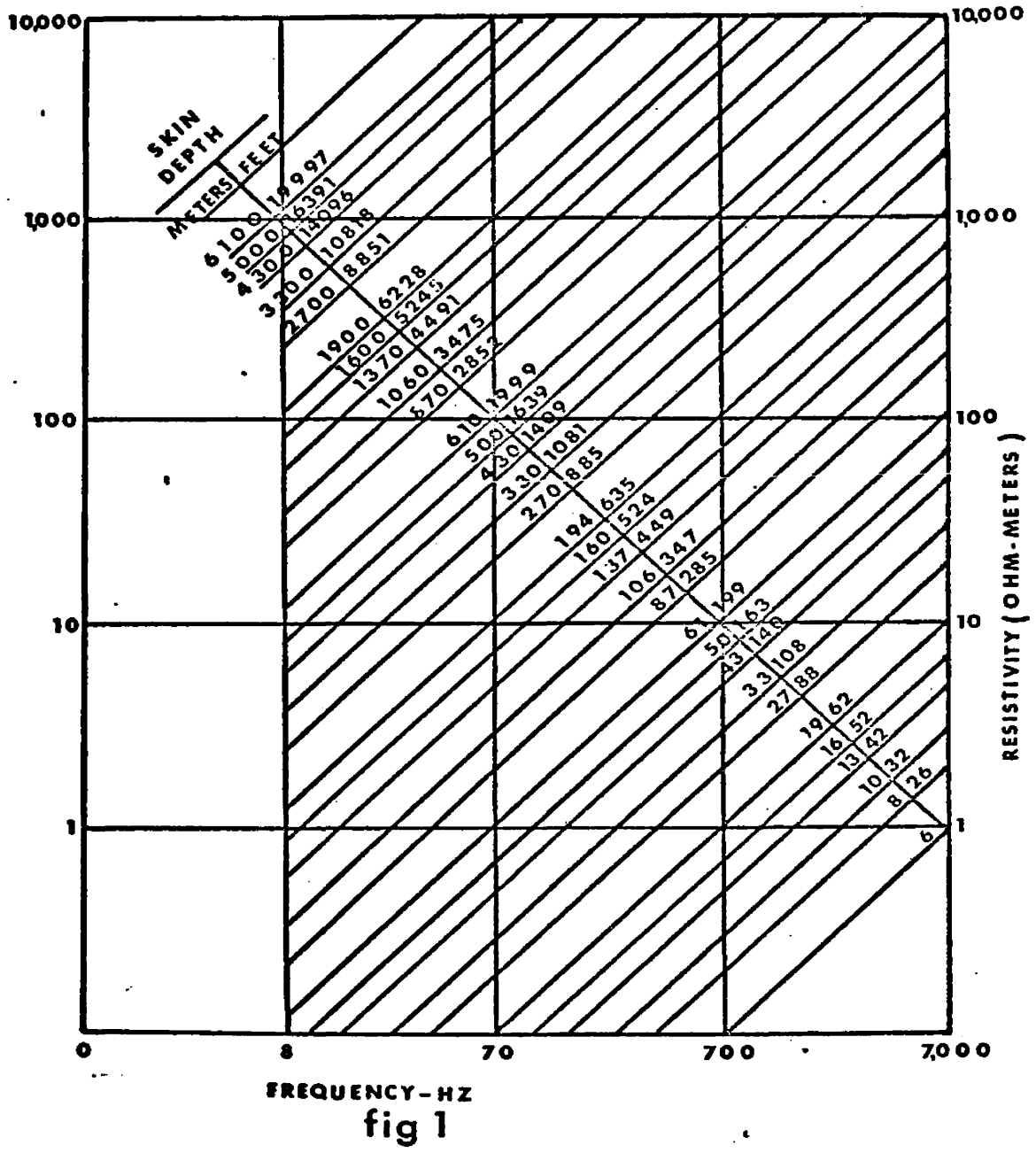

Figure 1. Graph showing skin depth vs frequency and resistivity.

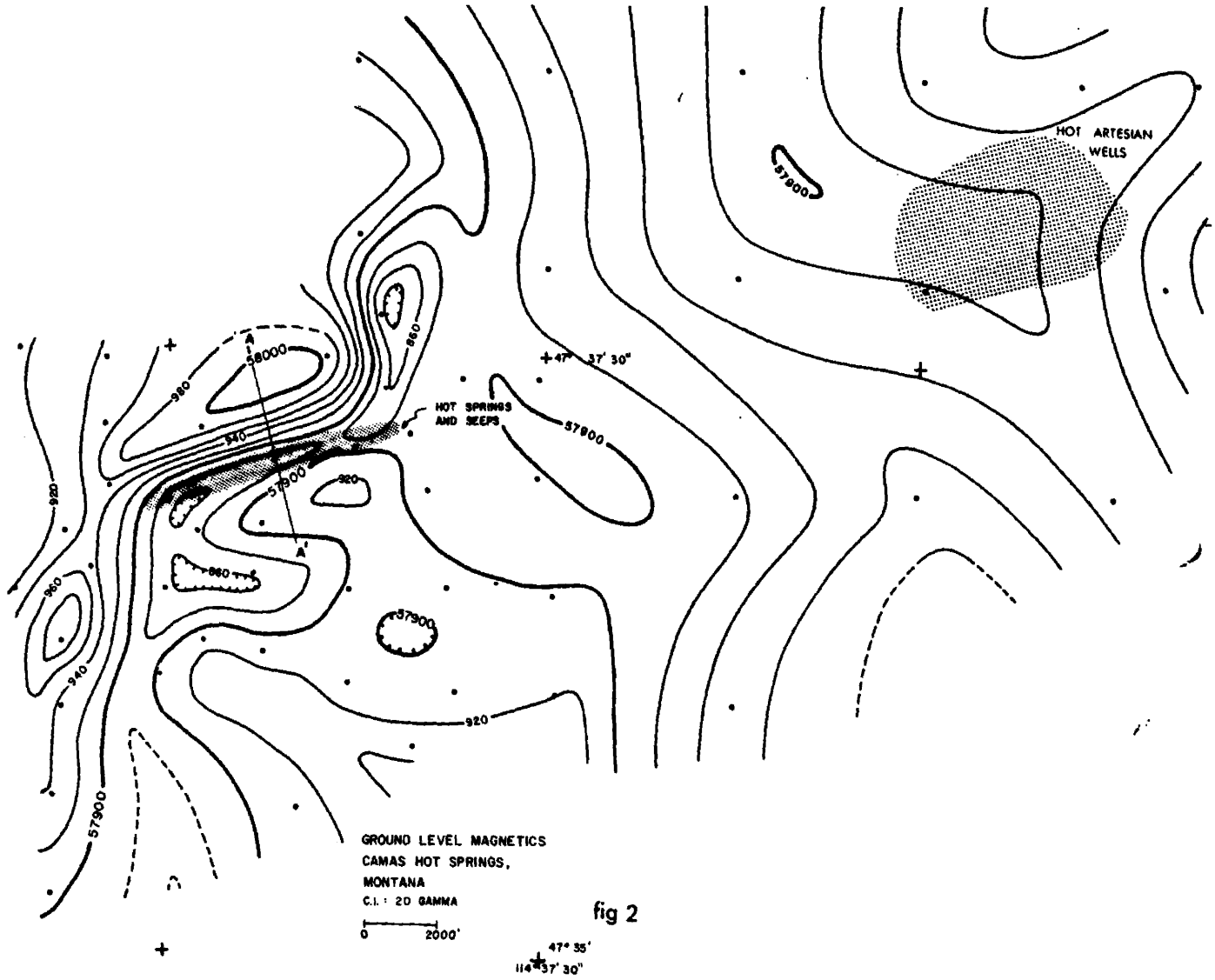

Figure 2. Ground level magnetics at Camas Hot Springs, Montana.

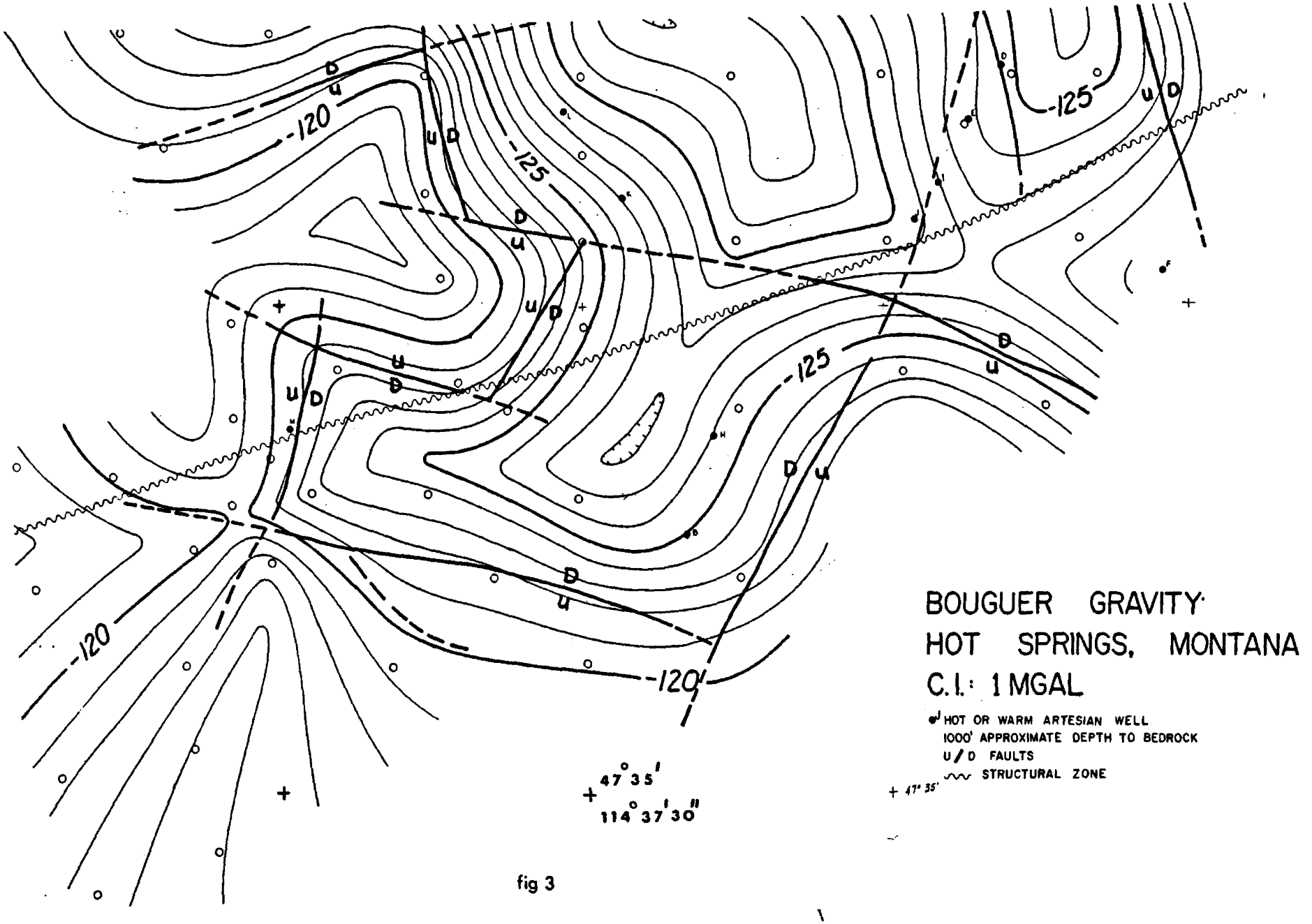

fig 3

Figure 3. Bouguer gravity map of Camas Hot Springs, Montana.

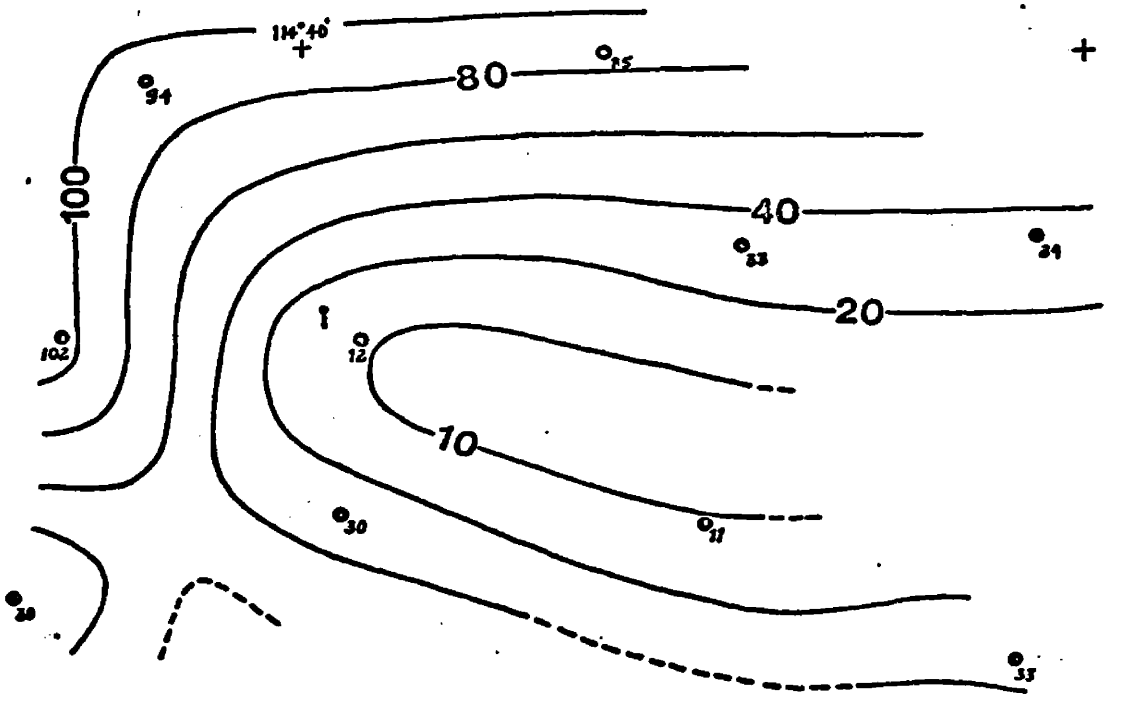

Figure 4. EM resistivity map of Camas Hot Springs, Montana.

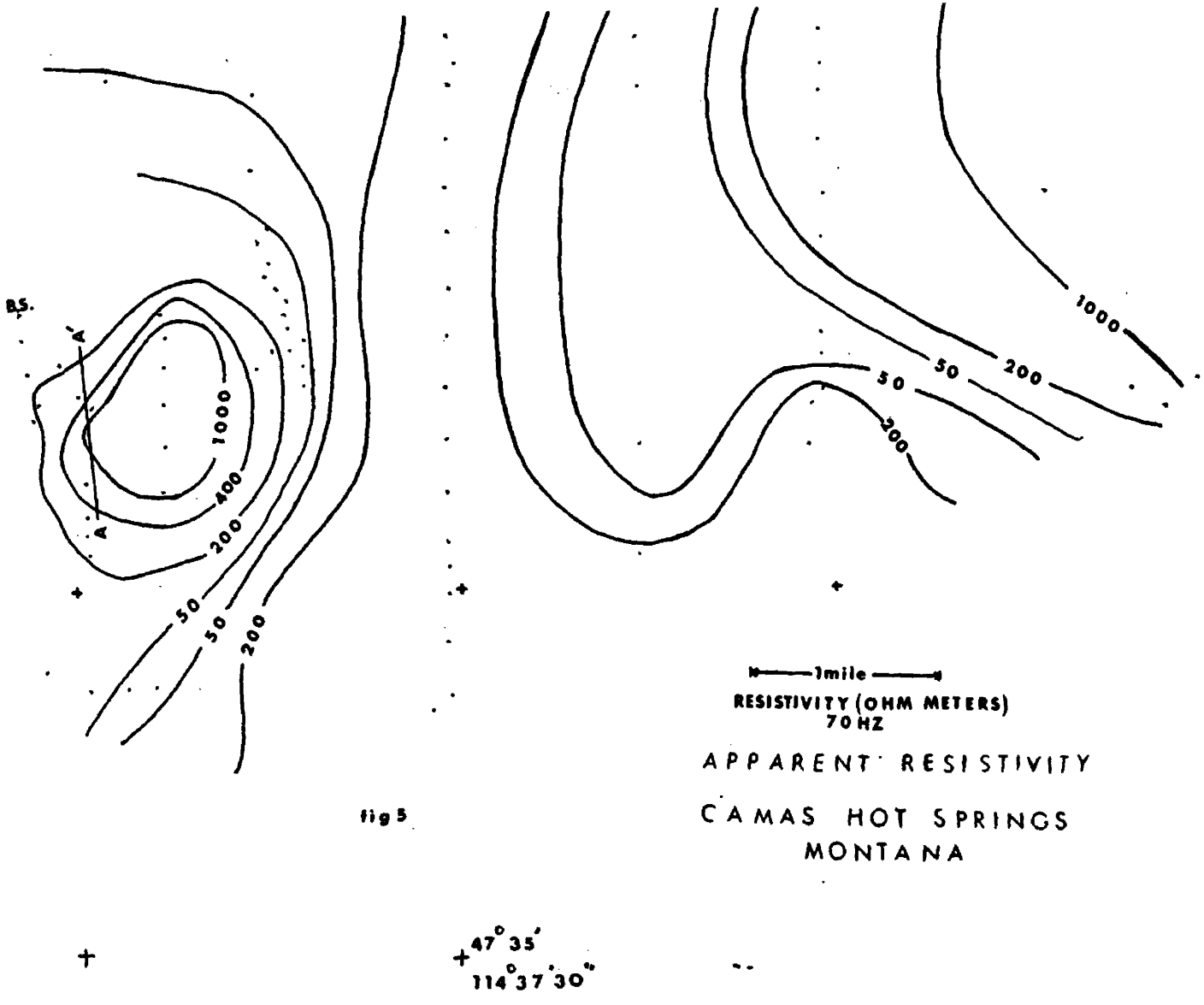

Figure 5. 70 Hz telluric apparent resistivity map of Camas Hot Springs, Montana.

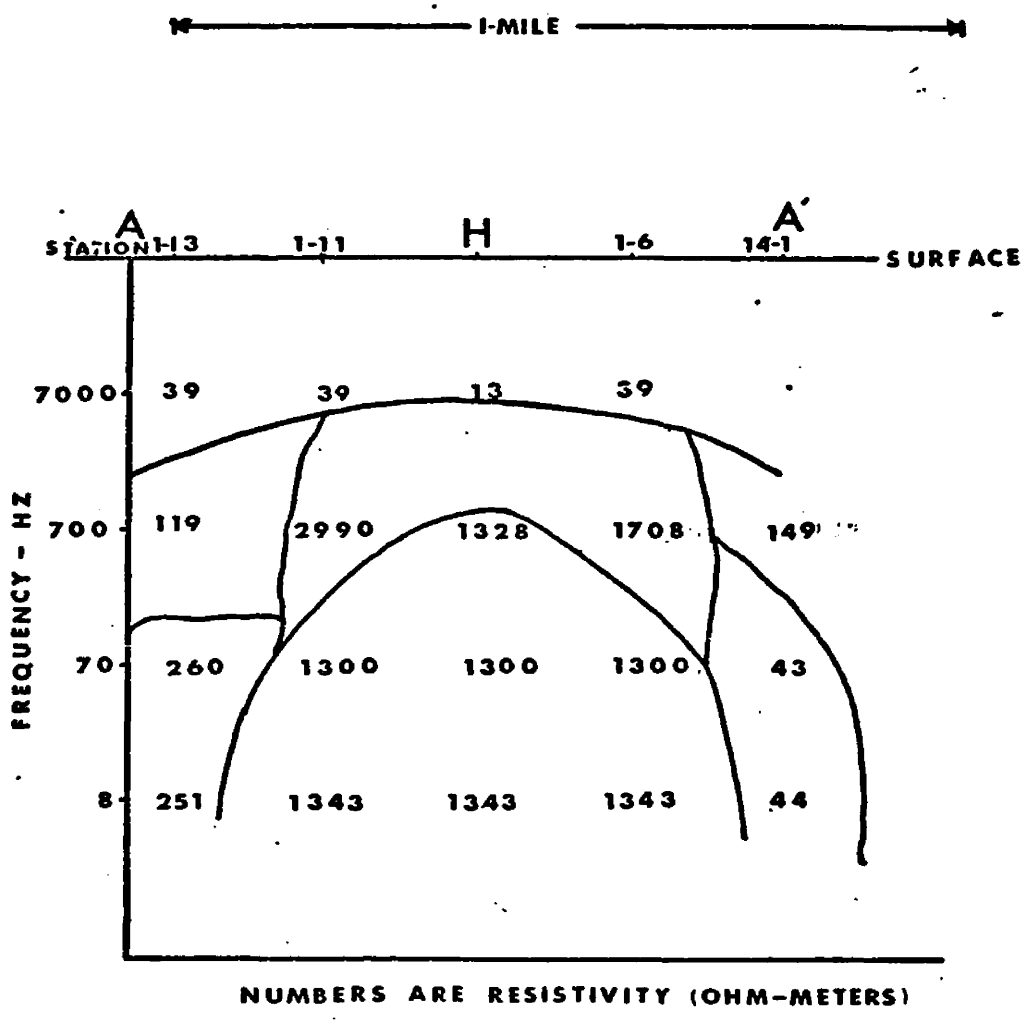

fig 6

Figure 6. Pseudo resistivity section showing apparent resistivity in ohm meters at different frequencies beneath cross section A-A' at Camas Hot Springs, Montana.

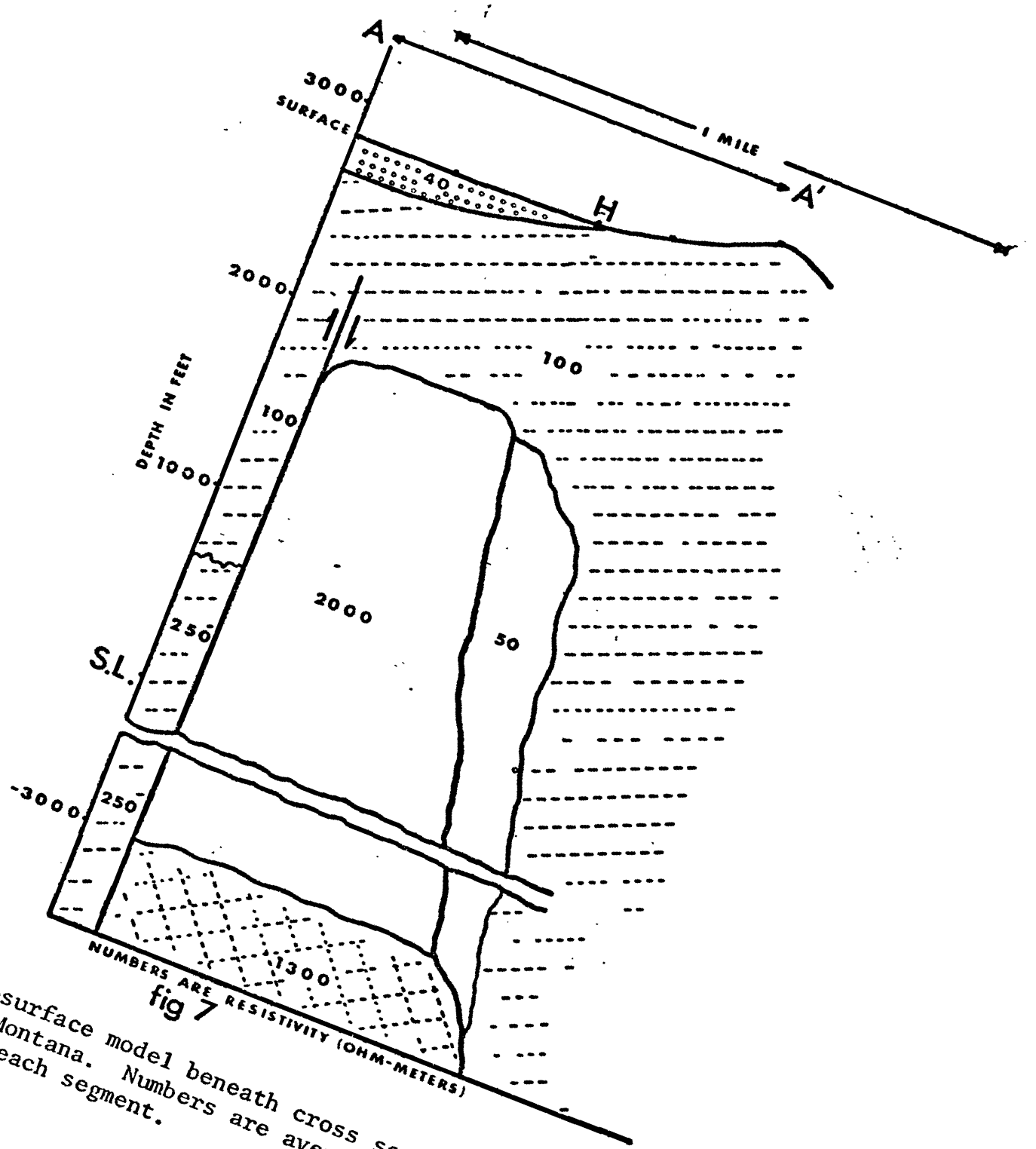

Figure 7. Subsurface model beneath cross section A-A' at Camas Hot Springs, Montana. Numbers are average apparent resistivity in ohm meters of each segment.

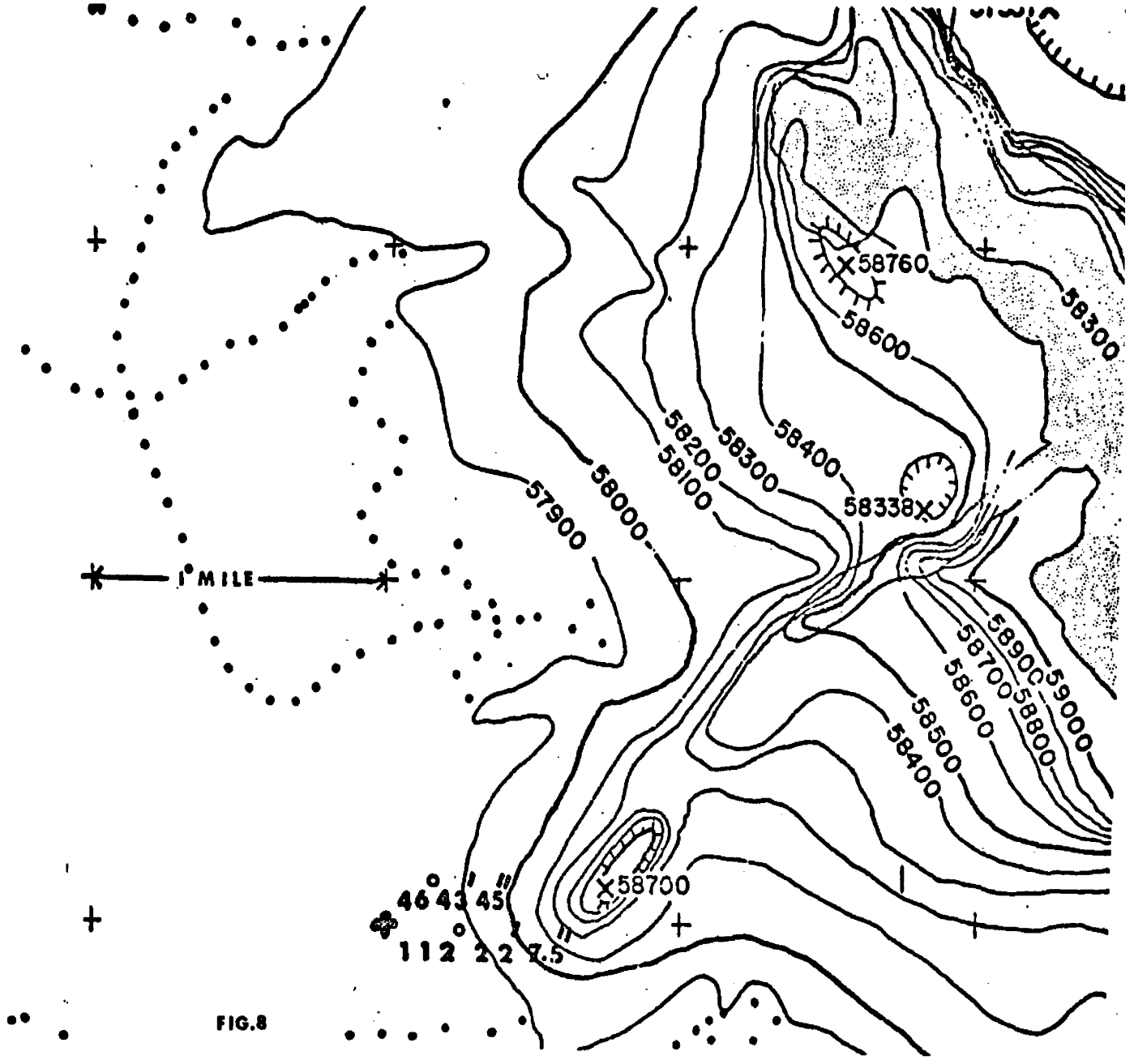

Figure 8. Ground total field intensity magnetic map of Marysville Geothermal Area. Contour interval 100 γ.

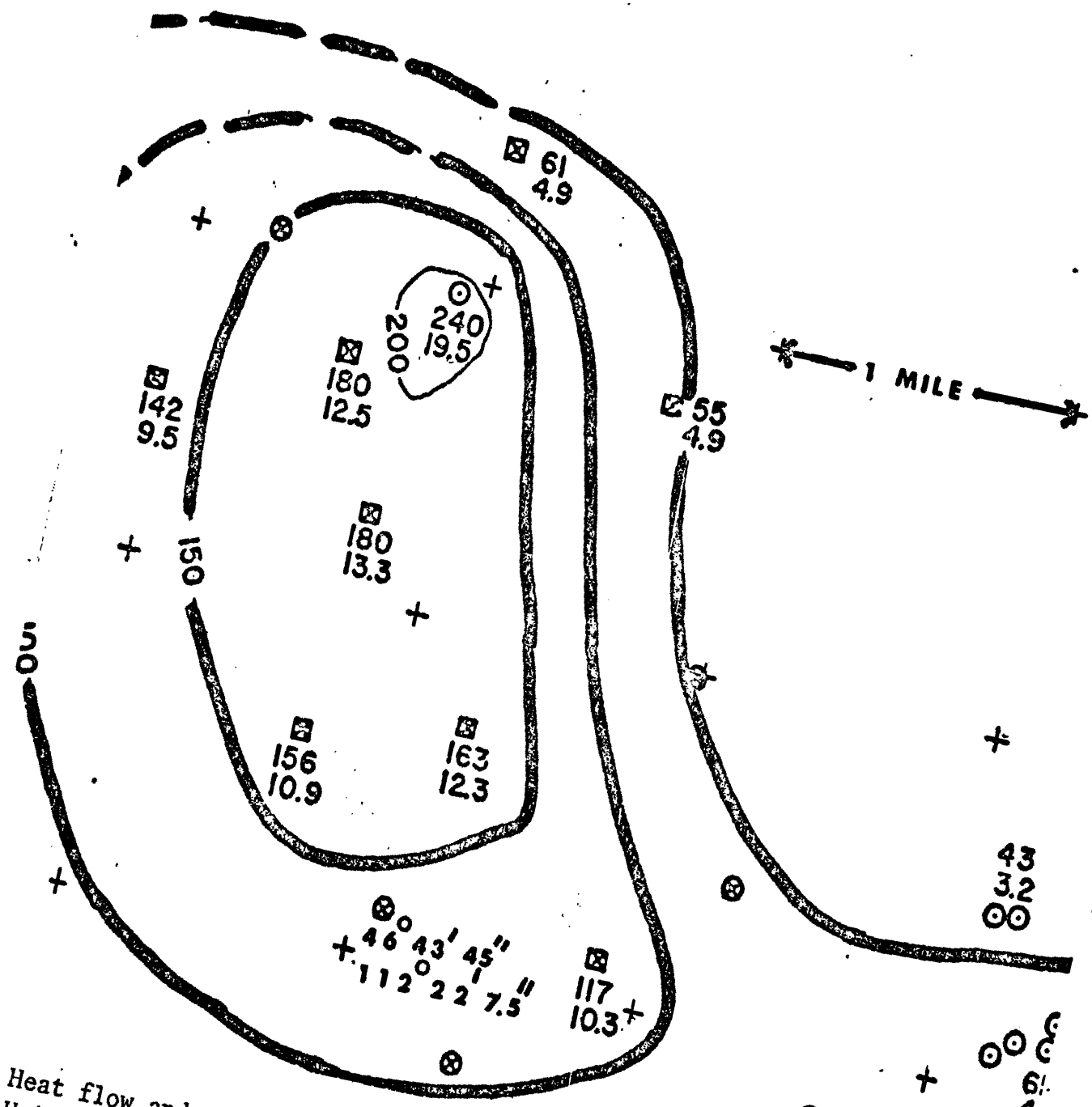

FIG. 9

Figure 9. Heat flow and geothermal gradients over Marysville Geothermal area. Units °C/km μcal/cm^{2}sec.

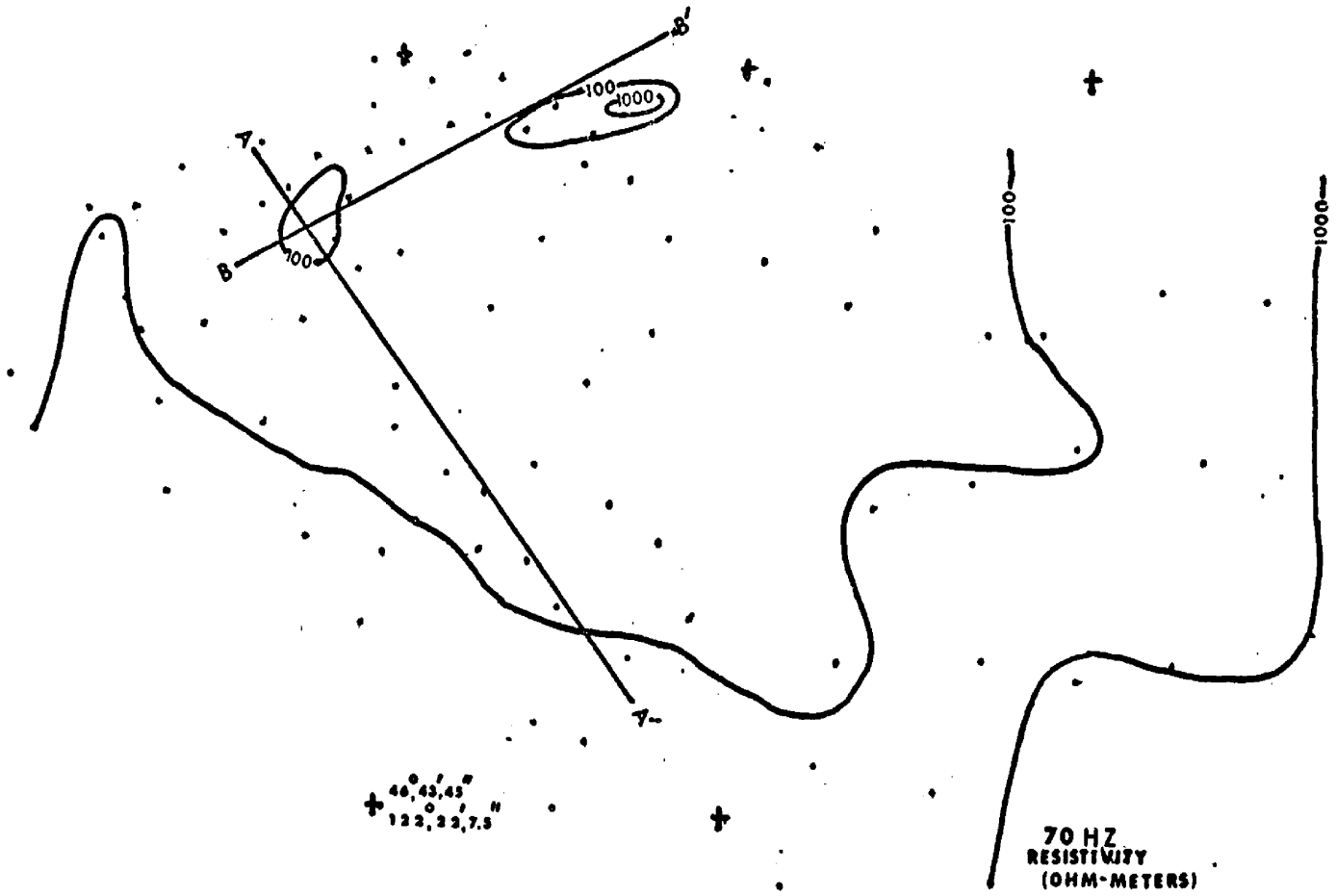

fig 10

Figure 10. 70 Hz telluric apparent resistivity map of Marysville Geothermal area.

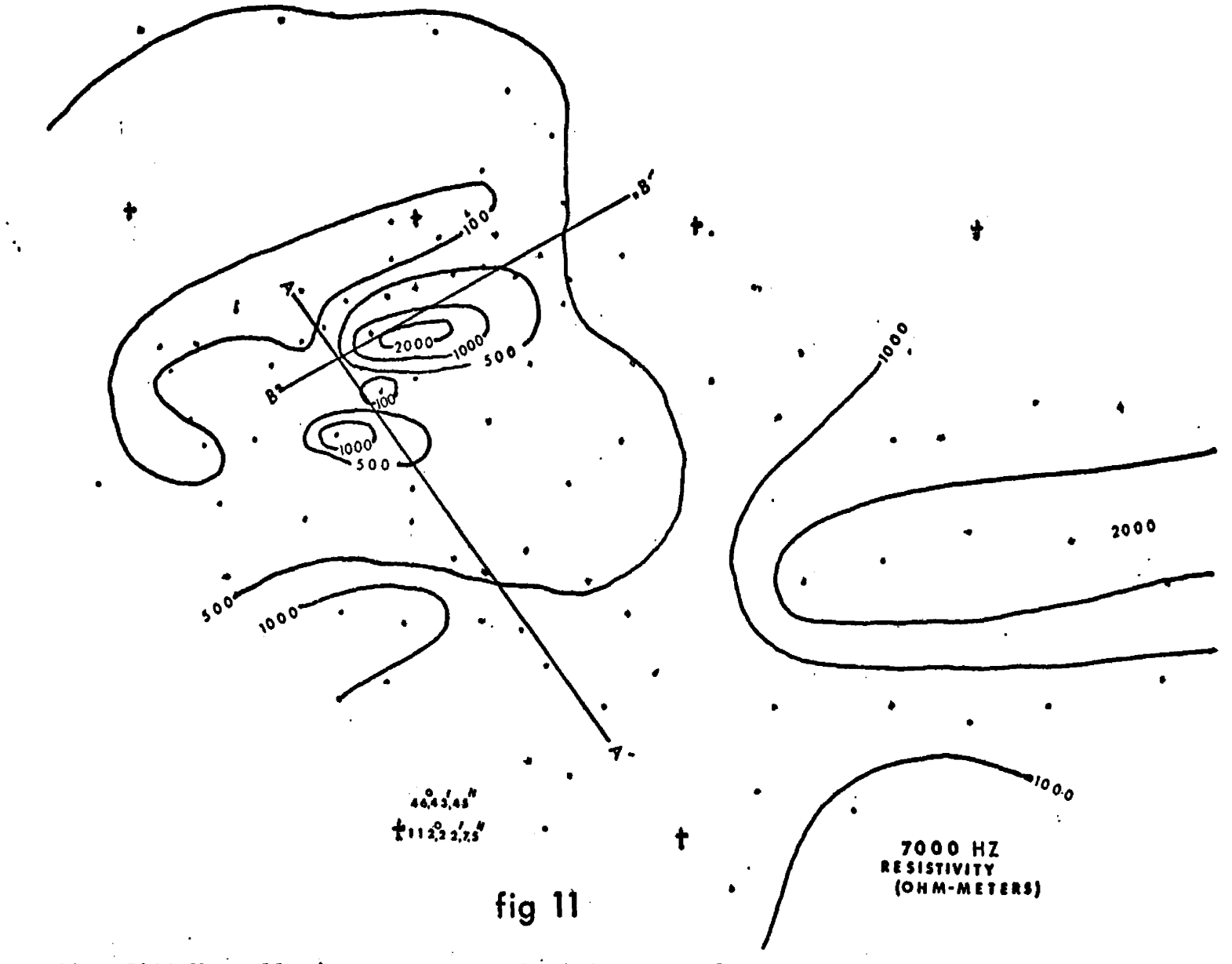

Figure 11. 7000 Hz telluric apparent resistivity map of Marysville Geothermal area.

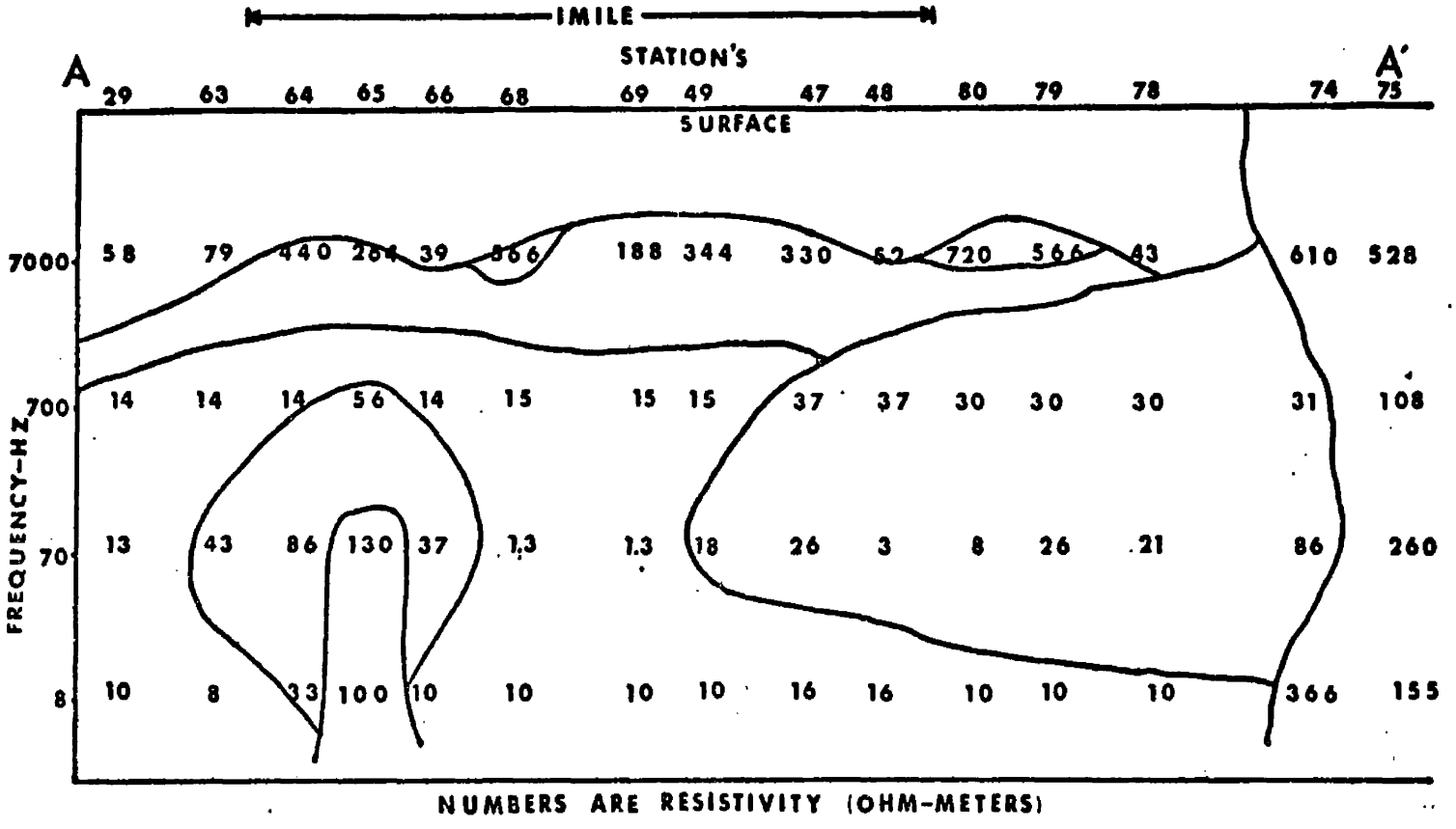

fig 12

Figure 12. Pseudo resistivity section showing apparent resistivity in ohm meters at different frequencies beneath cross section A-A' at the Marysville Geothermal area.

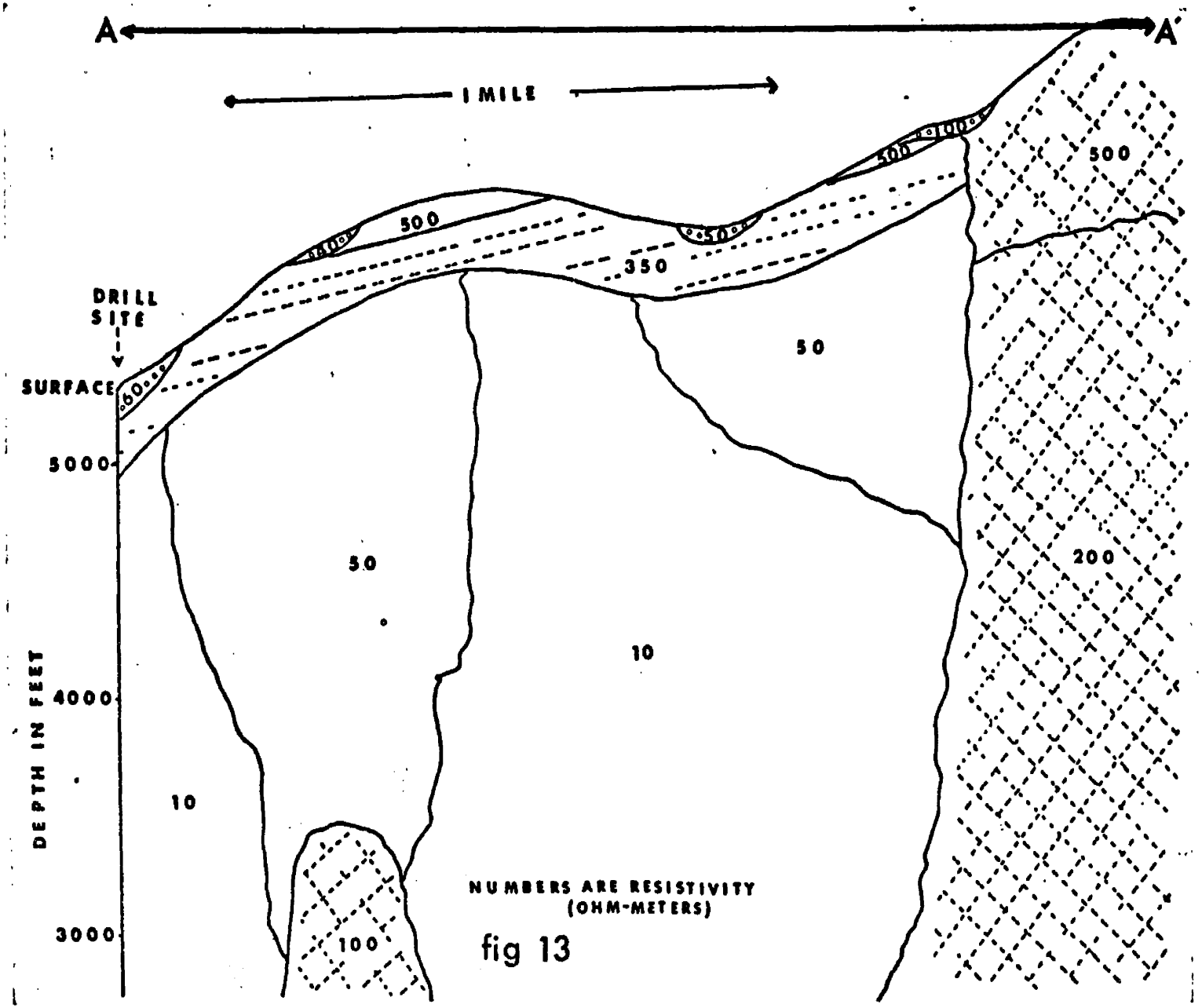

Figure 13. Subsurface structure model beneath cross section A-A' at the Marysville Geothermal area. Numbers are average apparent resistivity in ohm meters of each segment.

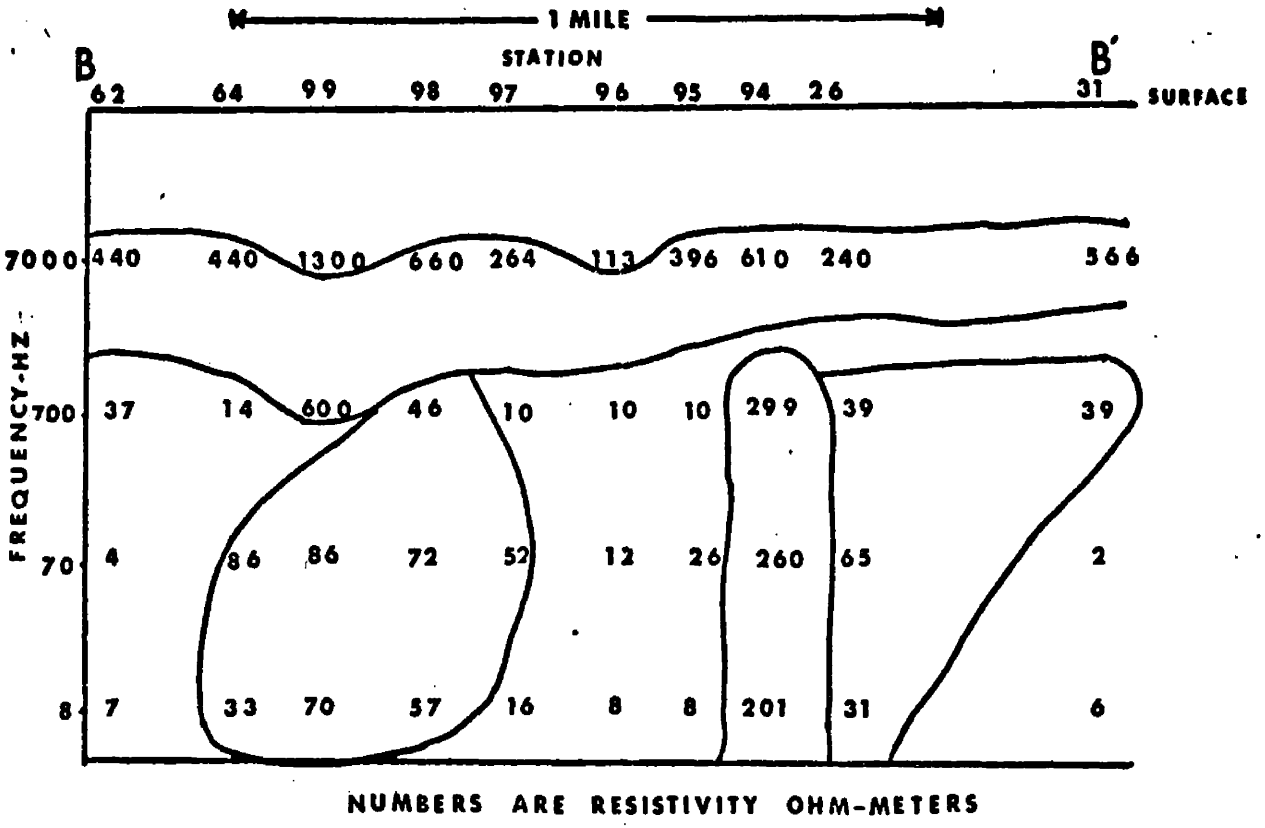

fig 14

Figure 14. Pseudo resistivity section showing apparent resistivity in ohm meters beneath cross section B-B' at the Marysville Geothermal area.

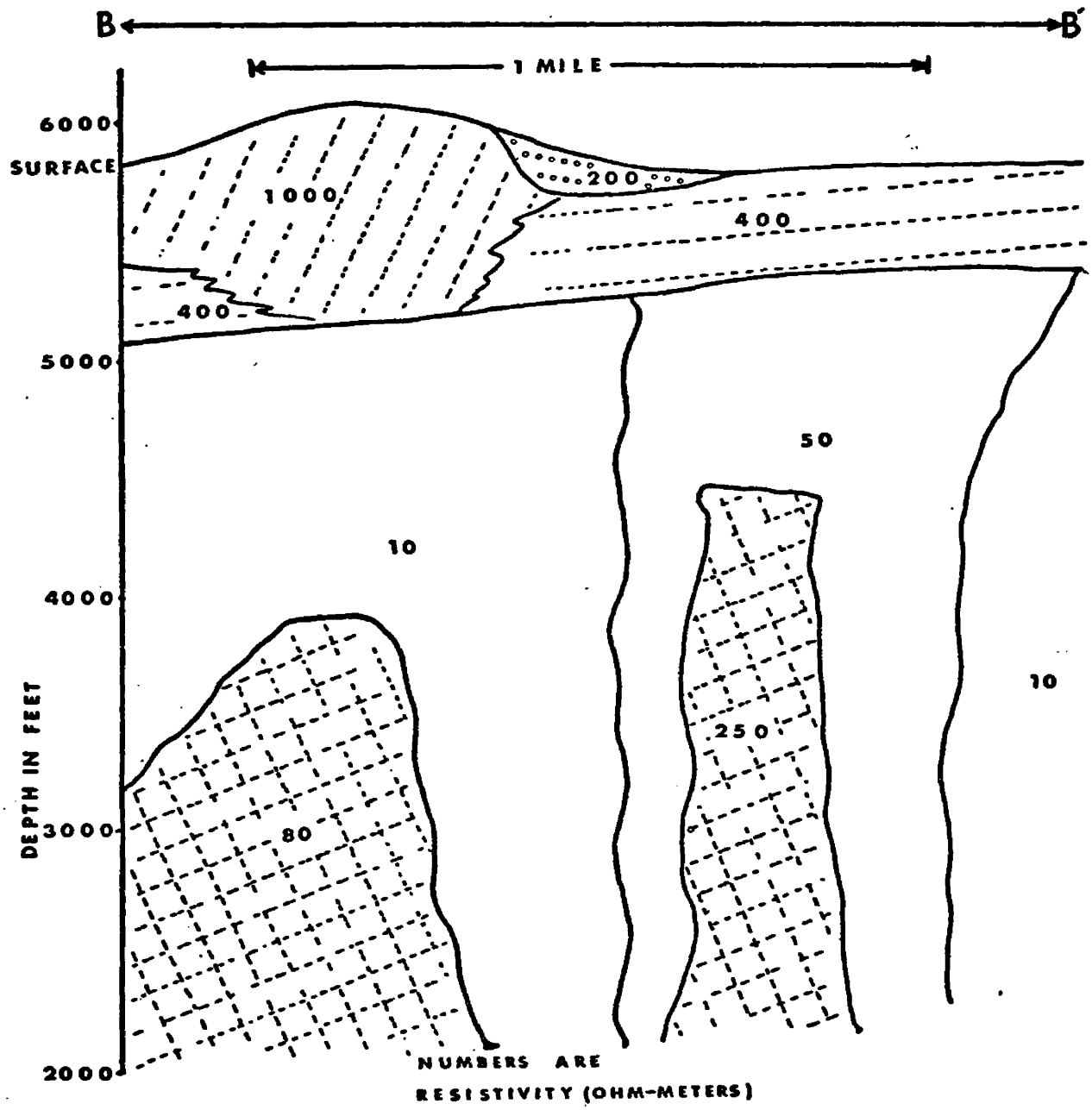

fig 15

Figure 15. Subsurface structure model beneath cross section B-B' at the Marysville Geothermal area. Numbers are average apparent resistivity in ohm meters of each segment.

APPENDIX B

TABLE OF PRINCIPAL FACTS

Hot Springs

Station No.	Latitude	Longitude	Time	ρa @70Hz
			sec	*ohm meters*
1A	47°37'23"	114°40'25"	1.3	100
2A	47°37'16"	114°40'25"	3.6	36
3A	47°37'10"	114°40'20"	1.8	72
4A	47°37'03"	114"40'20"	1.8	72
5A	47°37'00"	114°40'16"	1.2	108
6A	47°36'63"	114°40'14"	.6	216
7A	47°36'50"	114°40'10"	2.4	54
8A	47°36'48"	114°40'08"	.6	216
9A	47°36'45"	114°40'08"	.3	36
10A	47°36'40"	114°40'05"	.3	433
11A	47°36'35"	114°40'00"	.3	433
12A	47°36'30"	114°39'58"	.3	433
13A	47°36'24"	114°39'57"	.5	260
14A	47°36'17"	114°39'55"	.6	216
15A	47°36'13"	114°39'55"	.5	260
1B	47°39'35"	114°35'00"	2.5	52
2B	47°39'23"	114°35'00"	2.5	52
3B	48°39'12"	114°35'00"	2.5	52
4B	48°39'07"	114°35'00"	2.5	52
5B	48°39'00"	114°35'00"	2.5	52
6B	47°38'52"	114°35'00"	.5	260
7B	47°38'47"	114°35'00"	.5	260
8B	47°38'40"	114°35'00"	.5	260
9B	47°38'22"	114°35'00"	.5	260
10B	47°38'15"	114°35'00"	.5	260
11B	47°38'04"	114°35'00"	.5	260
12B	47°37'53"	114°35'00"	.5	260
13B	47°37'40"	114°35'00"	.5	260
14B	47°37'34"	114°35'00"	20.0	6.5
15B	47°36'55"	114°35'00"	20.0	6.5
16B	47°36'50"	114°35'00"	20.0	6.5
17B	47°36'38"	114°35'00"	.5	260
18B	47°36'30"	114°35'00"	.5	260
19B	47°36'25"	114°35'02"	.5	260
20B	47°36'17"	114°35'05"	.5	260

Station No.	Latitude	Longitude	Time *sec*	ρa @70Hz *ohm meters*
1C	47°39'35"	114°35'47"	1.5	86
2C	47°39'20"	114°35'47"	1.5	86
3C	47°39'07"	114°35'47"	1.5	86
4C	47°38'47"	114°35'47"	1.5	86
5C	47°38'40"	114°35'47"	4.0	32
6C	47°38'27"	114°35'47"	4.0	32
7C	47°38'15"	114°35'47"	4.0	32
8C	47°38'02"	114°35'47'	3.0	43
9C	46°37'50"	114°35'47"	3.0	43
10C	46°37'37"	114°35'47"	3.0	43
11C	46°37'17"	114°35'47"	30.0	4.3
12C	46°36'55"	114°35'47"	30.0	4.3
13C	46°36'40"	114°35'47"	30.0	4.3
14C	46°36'30"	114°35'47"	30.0	4.3
15C	46°36'17"	114°35'47"	.5	260
16C	46°36'05"	114°35'47"	.5	260
17C	46°35'40"	114°35'47"	.5	260
1D	47°38'40"	114°37'30"	.1	1300
2D	47°38'40"	114°37'30"	.1	1300
3D	47°38'20"	114°37'30"	.1	1300
4D	47°38'05"	114°37'30"	.1	1300
5D	47°37'50"	114°37'30"	.1	1300
6D	47°37'37"	114°37'30"	.1	1300
7D	47°37'22"	114°37'30"	.1	1300
8D	47°37'10"	114°37'30"	.1	1300
9D	47°36'55"	114°37'30"	.1	1300
10D	47°36'42"	114°37'30"	.1	1300
11D	47°36'30"	114°37'30"	.1	1300
12D	47°36'20"	114°37'30"	.1	1300
13D	47°36'07"	114°37'07"	.1	1300
14D	47°35'52"	114°37'07"	.1	1300
15D	47°35'40"	114°37'30"	.1	1300
1E	47°36'05"	114°38'50"	.5	260
2E	47°36'17"	114°38'50"	2.8	45
3E	47°36'30"	114°38'50"	.5	260
4E	47°37'00"	114°38'50"	.5	260
1F	47°36'05"	114°39'27"	.2	650
2F	47°36'20"	114°39'27"	.2	650
3F	47°36'25"	114°39'27"	.2	650
4F	47°37'05"	114°39'27"	.2	650
5F	47°37'40"	114°39'27"	.1	1300
6F	47°37'47"	114°39'27"	.1	1300

Station No.	Latitude	Longitude	Time	ρa @70Hz
			sec	*ohm meters*
1G	47°38'50"	114°40'05"	5	26
2G	47°38'50"	114°38'45"	8	16
3G	47°38'40"	114°38'45"	8	16
4G	47°38'10"	114°38'45"	2.5	52
5G	47°37'50"	114°38'45"	3	43
6G	47°37'40"	114°38'35"	3	43
7G	47°37'30"	114°38'35"	2	65
8G	47°37'20"	114°38'35"	2	65
9G	47°37'13"	114°38'30"	2	65
10G	47°37'10"	114°38'25"	2	65
11G	47°36'45"	114°38'20"	2	65
1H	47°35'50"	114°40'40"	1.5	86
2H	47°30'50"	114°40'17"	2	65
3H	47°30'45"	114°40'00"	2	65
4H	47°30'45"	114°39'45"	4	32
5H	47°30'45"	114°39'35"	3	43
1I	47°38'10"	114°34'30"	2	65
2I	47°37'05"	114°33'50"	12	10
3I	47°37'00"	114°33'20"	26	5
4I	47°37'00"	114°32'25"	.1	1300
5I	47°37'50"	114°33'20"	.1	1300
6I	47°38'20"	114°33'20"	.1	1300
7I	47°38'40"	114°33'20"	.1	1300
8I	47°38'45"	114°33'00"	.1	1300

TABLE OF PRINCIPAL FACTS

Marysville

tation No.	Latitude	Longitude	Time	ρa @70Hz	ρa @7000Hz
			sec	*ohm meters*	
1	46°43'55"	112°18'45"	.2	650	495
2	46°44'05"	112°19'10"	.9	144	720
3	46°44'05"	112°19'38"	.2	650	158
4	46°44'05"	112°20'00"	2.0	65	720
5	46°44'08"	112°20'25"	3.0	43	440
6	46°43'40"	112°20'30"	1.5	86	793
7	46°43'35"	112°20'35"	1.0	130	528
8	46°43'40"	112°20'05"	1.0	130	1321
9	46°44'25"	112°20'15"	1.5	86	3965
10	46°44'30"	112°19'55"	2.0	65	2643
11	46°44'35"	112°19'35"	14.0	9	2643
12	46°44'35"	112°19'10"	1.0	130	2643
13	46°44'35"	112°18'40"	.1	1300	7930
14	46°44'25"	112°18'30"	.1	1300	991
15	46°44'30"	112°18'20"	.1	1300	1982
16	46°44'47"	112°18'30"	.1	1300	793
17	46°44'55"	112°18'55"	.2	650	991
18	46°44'55"	112°19'25"	.6	216	793
19	47°44'50"	112°19'40"	1.0	130	1132
20	46°44'50"	112°19'55"	32.0	4	991
21	46°44'50"	112°19'25"	32.0	4	305
22	46°44'55"	112°20'45"	9.0	14	793
23	46°45'02"	112°21'05"	2.0	65	113
24	46°45'10"	112°21'20"	130.0	1	720
25	46°45'15"	112°21'25"	130.0	1	720
26	46°45'20"	112°21'32"	2.0	65	240
27	46°45'20"	112°21'50"	10.0	13	62
28	46°45'22"	112°22'20"	6.0	21	72
29	46°45'10"	112°22'35"	10.0	13	58
30	46°45'20"	112°21'10"	.1	1300	417
31	46°45'30"	112°21'10"	65.0	2	566
32	46°45'22"	112°20'40"	6.0	21	991
33	46°45'15"	112°20'30"	21.0	6	566
34	46°45'05"	112°20'20"	8.0	16	440
35	46°45'35"	112°21'48"	5.0	26	180
36	46°45'40"	112°21'27"	65.0	2	158
37	46°45'45"	112°21'40"	130.0	1	123
38	46°45'52"	112°22'05"	26.0	5	141
39	46°45'55"	112°22'28"	6.0	21	793
40	46°45'55"	112°22'40"	130.0	1	146
41	46°45'52"	112°23'20"	16.0	8	495
42	46°45'10"	112°22'52"	4.0	32	93
43	46°45'05"	112°23'15"	65.0	2	72
44	46°44'40"	112°23'00"	4.0	32	39
45	46°44'25"	112°22'50"	1.0	130	264
46	46°44'20"	112°22'25"	1.0	130	1321

tation No.	Latitude	Longitude	Time	ρa @70Hz	ρa @7000Hz
			sec	*ohm meters*	
47	46°44'30"	112°21'50"	5.0	26	330
48	46°44'32"	112°21'45"	43.0	3	52
49	46°44'35"	112°22'05"	7.0	18	344
50	46°44'45"	112°22'25"	3.0	37	1132
51	46°44'35"	112°22'30"	130.0	1	152
52	46°45'05"	112°24'20"	10.0	12	165
53	46°44'50"	112°24'10"	8.0	16	440
54	46°44'35"	112°24'13"	13.0	10	377
55	46°44'05"	112°24'13"	21.0	6	198
56	46°44'20"	112°24'00"	13.0	10	146
57	46°44'35"	112°23'25"	10.8	12	226
58	46°44'50"	112"23'50"	18.0	7	220
59	46°45'10"	112°24'15"	130.0	1	566
60	46°45'12"	112°23'45"	8.0	16	100
61	46°44'45"	112°22'40"	32.0	4	396
62	46°45'00"	112°22'40"	32.0	4	440
63	46°45'05"	112°22'34"	3.0	43	79
64	46°45'05"	112°22'30"	1.5	86	440
65	46°44'57"	112°22'30"	1.0	130	264
66	46°44'55"	112°22'25"	3.5	37	39
67	46°44'55"	112°22'22"	8.0	16	180
68	46°44'40"	112°22'10"	130.0	1	566
69	46°44'35"	112°22'05"	130.0	1	188
70	46°44'30"	112°21'30"	65.0	2	61
71	46°44'25"	112°21'15"	10.0	13	113
72	46°44'20"	112°21'10"	7.0	18	528
73	46°44'10"	112°21'00"	3.5	37	881
74	46°44'05"	112°21'15"	1.5	86	610
75	46°44'00"	112°20'20"	.5	260	528
76	46°43'40"	112°21'30"	.5	260	793
77	46°43'45"	112°21'35"	.5	260	528
78	46°44'10"	112°21'30"	6.1	21	113
79	46°44'15"	112°21'35"	5.0	26	566
80	46°44'15"	112°21'40"	16.0	8	720
81	46°44'15"	112°22'05"	1.2	108	1982
82	46°44'05"	112°22'10"	.8	162	793
83	46°44'40"	112°23'00"	1.0	130	330
84	46°44'50"	112°23'05"	1.0	130	344
85	46°45'00"	112°23'20"	1.5	86	528
86	46°45'05"	112°23'00"	4.0	32	52
87	46°45'05"	112°22'42"	3.5	37	305
88	46°45'07"	112°22'30"	7.2	18	226
89	46°45'12"	112°22'25"	16.2	8	105
90	46°45'20"	112°22'10"	5.0	26	113

Station No.	Latitude	Longitude	Time	ρa @70Hz	ρa @7000Hz
			sec	*ohm meters*	
91	46°45'20"	112°22'00"	6.0	21	63
92	46°45'22"	112°21'40"	3.5	37	74
93	46°45'10"	112°21'22"	5.0	26	158
94	46°45'17"	112°21'35"	.5	260	610
95	46°45'17"	112°21'37"	5.0	26	396
96	46°45'17"	112°21'55"	4.0	32	113
97	46°45'10"	112°22'05"	2.5	52	264
98	46°45'10"	112°22'10"	1.8	72	660
99	46°45'05"	112°22'15"	4.8	27	2643
100	46°45'02"	112°21'57"	130.0	1	5286